LAND COVER CLASSIFICATION CONCEPT FOR ANISOTROPY CORRECTION IN HYPERSPECTRAL IMAGERY

J. Weyermann [a], D. Schläpfer [b], A. Hueni [a], M. Kneubühler [a], K.I. Itten [a]

[a] RSL, University of Zurich, Winterthurerstr. 190, 8057 Zurich, Switzerland
[b] ReSe Applications Schläpfer, Langeggweg 3, 9500 Wil, Switzerland

ABSTRACT:

An empirical (target-) BRDF normalization method has been implemented for hyperspectral data processing, following the approach of Kennedy, published in 1997. Correction results of this method highly depend on the successful application of an appropriate spectral pre-classification which necessarily must be insensitive to reflectance anisotropy.
A standard classification output (as of ATCOR-4) is first evaluated for its suitability concerning anisotropy normalization. A hierarchical BRDF selection scheme is then set up, covering the most prominent target classes in the image. A classification algorithm is then evaluated on the basis of a standard spectral angle mapper (SAM) approach with the RSL's spectral database SPECCHIO attached for reference spectra evaluation. Results show that the ATCOR-4 pre-classification output is highly sensitive to the reflectance anisotropy and therewith not suited for pre-classification. The SAM pre-classification is still under investigation, but first tests using reference spectra out of the reflectance data itself showed problems *due to* the high robustness against brightness differences since a gradient must be estimated from targets of comparable brightness.

1. INTRODUCTION

Anisotropic reflectance behaviour is typical for most natural surfaces. Assuming a given fixed illumination direction and homogeneous target, the reflected energy measurable by a sensor changes with varying sensor angular position. Likewise, the received energy for a sensor at fixed position depends on the illumination direction. The target- and wavelength-specific characteristics of this physical phenomenon may be expressed by the conceptual quantity of the bi-directional reflectance distribution function (BRDF). Derived quantities like the bi-directional reflectance factor (BRF) are commonly used to describe the reflectance anisotropy, which in turn enables the estimation of e.g. structural variables of the specific target the sensor looked at.

However, often reflectance anisotropy is considered as an interfering effect in airborne or space borne imaging spectrometer data. Changes in across-track radiometry, which are caused by the sensor look angle variation, lead to misclassification or false estimation of surface properties. With increasing accuracy of methods for atmospheric correction, the relative errors caused by reflectance anisotropy become even more severe.

A number of methods exist to overcome this problem. Purely empirical, scene based methods may serve as fast, automated correction procedure of target induced reflectance anisotropy. Due to the strong coherence between target properties and reflectance anisotropy, empirical approaches like the band-specific quadratic curve fitting

method, which was first used by Leckie (Leckie 1987) and evaluated by Kennedy (Kennedy et al 1997) rely on a proper spectral pre-classification. This classification procedure must necessarily be highly insensitive to the reflectance anisotropy occurring in the data; its class definition must be designed in a way that it can discern reflectance differences caused by cross-track reflectance anisotropy and those caused by within-class variation that also would be visible under constant illumination and sensor angles. The goal of the present study is to investigate the potential of spectral classification algorithms to provide a set of spectral classes, which have to be distinguished in imaging spectroscopy data in order to perform an empirical normalisation of reflectance anisotropy. A standard spectral classification procedure (SPECL algorithm) is used first as a pre-classification and its performance is evaluated with a HyMap dataset taken in 2004 over the "Vordemwald" test site in northern Switzerland. In a second step, the Spectral Angle Mapper (SAM) algorithm is used with reference spectra extracted from the image data.

2. METHODS

Three overlapping datasets have been acquired at the "Vordemwald" test site in northern Switzerland, two of which are taken in parallel in north-south direction with an overlap of a few hundred meters (VDW1, left and VDW2, right). One data set has been recorded perpendicular, therewith scanning in the so-called sun principle plane. This dataset has not been taken into account for the current investigation.

The HyMap Imaging Spectrometer is acquiring 512 pixels per scan line with 126 spectral bands recorded simultaneously between 400 and 2500 nm, with a FOV of 61.3°. The data were taken from an operating altitude of 2500m above ground; this results in a spatial resolution of 7.2 m in along-track and 6.0 m in across-track direction. All image data have been resampled during the parametric geometric correction process following PARGE (Schläpfer 2003) and (Schläpfer and Richter 2002) to an effective squared pixel size of 5x5 m. Atmospheric correction has been carried out using the ATCOR-4 software (Richter 2008) with a rural standard atmosphere. Remaining reflectance anisotropy in the data may then be attributed to the target specific directional reflectance behaviour exclusively. Topographic effects can be neglected due to the rather flat terrain. The SPECL classification algorithm as implemented in the

not classified | mix of veget./soil | dry veg. / soil
clear water | bare soil (dark) | sparse veg. / soil
dark vegetation | bare soil | bright sand
avg. vegetation | asphalt/dk sand | cloud
bright vegetation | sand / bare soil | turbid water
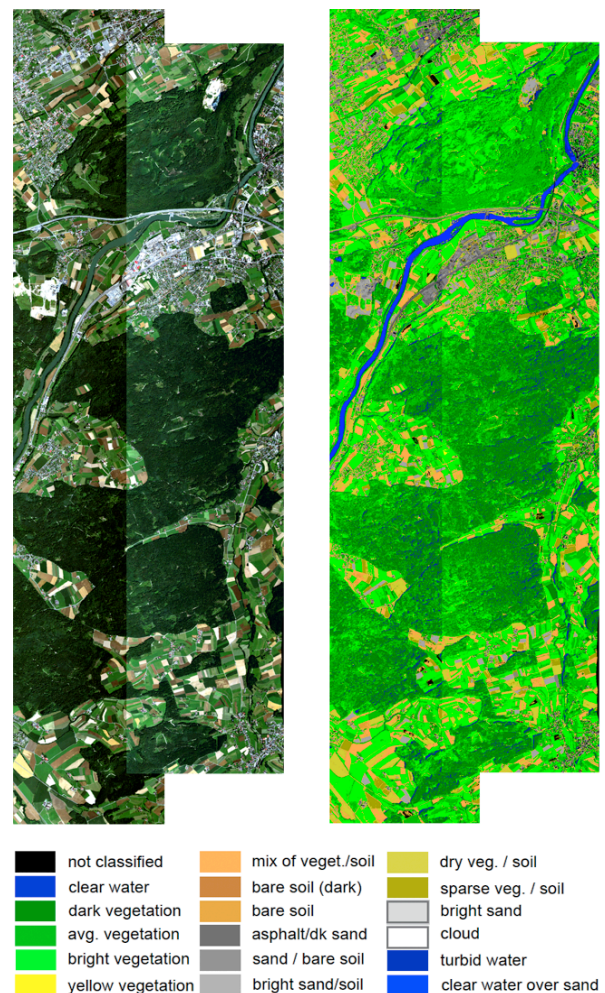yellow vegetation | bright sand/soil | clear water over sand

Figure 1: Mosaicked HyMap data (R,G,B = HyMap Band 14,8,2), left; SPECL classification result (right).

ATCOR-4 software package has been used to derive a spectral pre-classification of the data, using the software's standard template spectra. 18 classes have been identified; however, only the dominating 3 vegetation classes have been taken into account for this study. Figure 1 shows the mosaicked HyMap data and the classification results. It is clearly visible, that the brightness gradient in the HyMap data results in a partial misclassification. The transition of the overlapping image strips is recognizable in the image data.

Empirical, scene-based BRDF normalization has been carried out following the means of Kennedy (Kennedy, Cohen et al. 1997).

Using the previously generated classification, a mean radiance by view angle calculation is performed, per spectral class and waveband, assuming that directional effects are zero when the view angle is zero. A quadratic model, which optimizes the residual error in a least-squares sense, is then fit to the data.

After an offset correction of the fitted mean reflectance at nadir to the *apparent* reflectance at nadir, the coefficients are transformed into a correction factor per view angle (respective column number).

This correction factor can be calculated and applied either in a multiplicative or additive manner. Due to the better performance that was evaluated in studies carried out by other authors (Schiefer, Hostert et al. 2006) only the multiplicative approach has been followed.
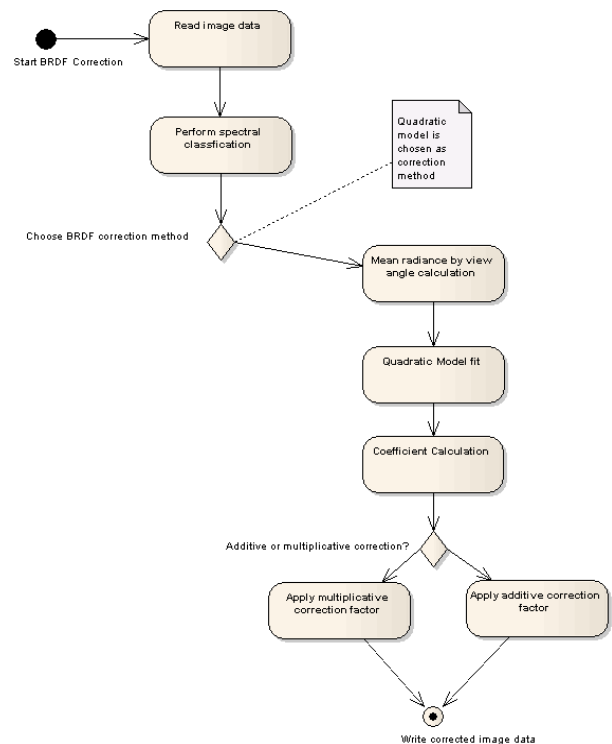

Figure 2: Workflow of the quadratic curve fitting process.

3. RESULTS

3.1 Results for SPECL pre-classification

Normalization of reflectance anisotropy is essential in order to enable accurate, quantitative data analysis, like the estimation of vegetation parameters (e.g. bio-chemicals content of tree species). The evaluation of the normalization results therefore focuses on green vegetation, which covers more than 70% of the data set under investigation. In the visual wavelength region (compare with Fig. 1) a severe brightness gradient can be observed primarily in forested areas. Figures 3, 4, 5 and 6 show the gradient that is observable in the data before and after correction, for the VDW 1 and VDW2 scenes, respectively. While for VDW1 the gradient is reduced by a noticeable amount, in the VDW2 case the correction is absolutely inappropriate to the observed gradient. The reason for this is the large within-class variation, especially for the "dark vegetation" class.

Figure 3: Brightness gradient in the VDW1 subset before correction.

Figure 4: Remaining gradient in the VDW1 subset after correction.

Figure 5: Brightness gradient in the VDW2 subset before correction.

Figure 6: Remaining gradient in the VDW2 subset after correction.

Figure 7 shows the SPECL classification results for the major vegetation classes (dark, average and bright vegetation), for the VDW1 scene. While the "dark vegetation" class covers mainly forest, and "bright vegetation" is related to pasture areas or crops, the "average vegetation" class seems to cover both of them. All of these classes show the typical reflectance curve for green vegetation, with varying total values in apparent surface reflectance, reaching from 25% (dark vegetation) up to 55% (bright vegetation) in the wavelength region around 1050 nm (HyMap band 42).

Figures 8 and 9 compare the column-wise averaged apparent surface reflectance for the visible, for the VDW1 and VDW2 case, and the "dark forest" class. The observed across-track changes in mean reflectance in the VDW2 dataset are similar for the other vegetation classes. There is no continuous decrease in reflectance from the left to the right. The reason for this is that the variance in apparent reflection caused by varying target properties is masked by the variation through reflectance anisotropy for a single target. This is not a surprising result. The investigated classification method is sensitive to reflectance anisotropy and therefore not suited as a pre-classification method for anisotropy correction.

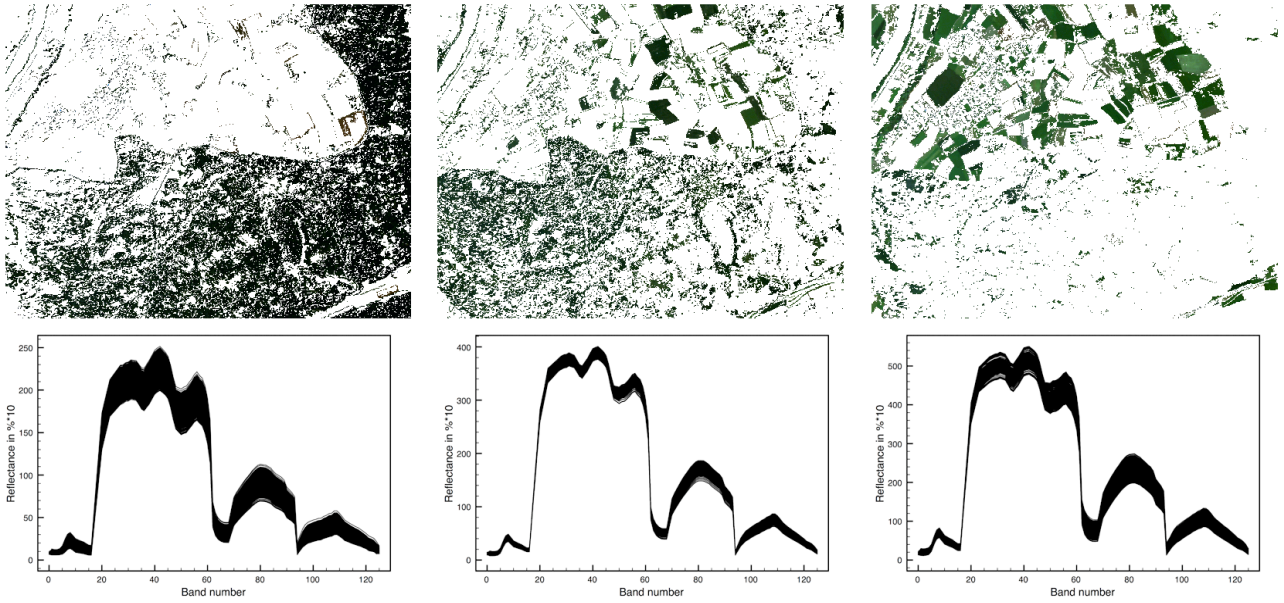Figures 10 and 11 illustrate the derived correction factors for VDW1 and VDW2.

Figure 7: SPECL classification result for the dominant vegetation classes (dark vegetation, left; average vegetation, middle; bright vegetation, right) demonstrated with a subset of the VDW1 scene, and spectra assigned to the respective classes.
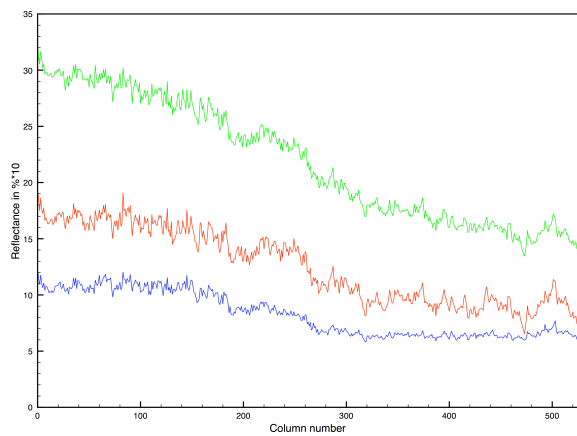

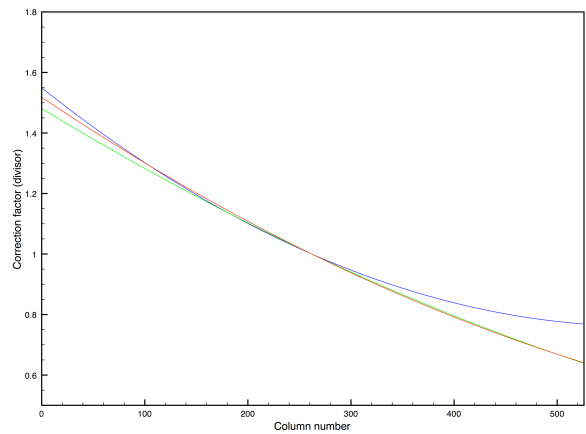Figure 8: Column-wise averaged reflectance for class "dark vegetation", VDW1 scene.

Figure 10: Calculated correction factors for class "dark vegetation", VDW1 scene.
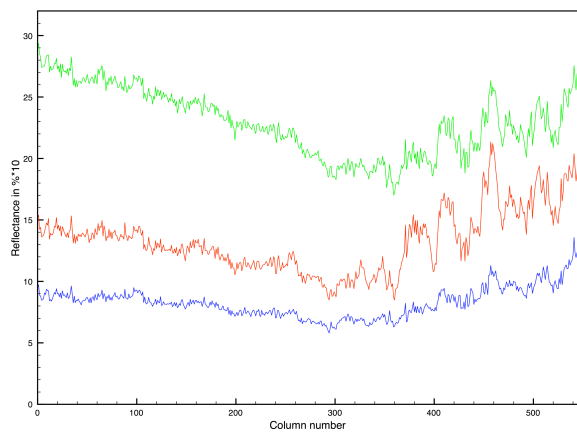

Figure 9: Column-wise averaged reflectance for class "dark vegetation", VDW2 scene.
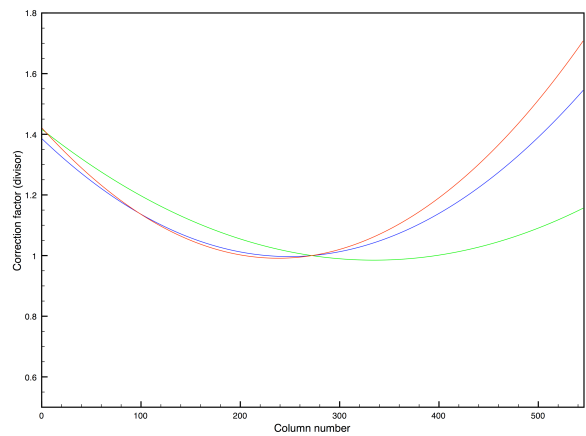

Figure 11: Calculated correction factors for class "dark vegetation", VDW2 scene.

3.2 Preliminary results for SAM pre-classification

A series of tests has been carried out for the "dark vegetation" case, using reference spectra derived from the real image data at various locations within forested areas, at nadir position. While the total illumination by definition does not play a role for the classification result, a key parameter seems to be the maximum allowed deviation from the reference angle. However, first preliminary results show that the advantages of the SAM (illumination insensitive classification) seem to become a drawback for the specific purpose of this application. The brightness gradient has to be estimated from a target class under the assumption that brightness differences are only caused by the reflectance anisotropy. The SAM algorithm is possibly too insensitive to distinguish between different target species that exhibit a very similar (vegetation) reflectance curve with only the illumination intensity being a discriminating factor. A combination of an illumination-sensitive classification method with the SAM might support the estimation of a class-wise brightness gradient.

4. CONCLUSIONS

A satisfactory target-BRDF normalization result for the case of (dark) vegetation could not be achieved so far. Both the SPECL algorithm and the SAM were not able to provide a spectral classification result that is both sensitive enough to the total illumination intensity (which is necessary for proper brightness gradient estimation) and insensitive to the within-class reflectance anisotropy.

The potential of the SAM algorithm, however, has not yet been fully investigated. Better results are possibly attainable with a modified set of reference spectra, and the use of spectrometer measurements taken in the field could have a positive influence.

In addition, the possibility of using SAM in combination with the SPECL algorithm will be a topic for further research.

6. REFERENCES

Kennedy, R. E., W. B. Cohen, et al. (1997). "Empirical Methods To Compensate for a View-Angle-Dependent Brightness Gradient in AVIRIS Imagery." Remote Sensing of Environment **62**: 277-291.

Leckie, D. G. (1987). "Factors affecting defoliation assessment using airborne multispectral scanner data." Eng. Remote Sensing **53**(12): 1665-1674.

Richter, R. (2008). Atmospheric/topographic correction for airborne imagery: ATCOR-4 User Guide. Wessling, Germany, DLR.

Schiefer, S., P. Hostert, et al. (2006). "Correcting brightness gradients in hyperspectral data from urban areas." Remote Sensing of Environment **101**: 25-37.

Schläpfer, D. (2003). Parametric Geocoding, User Guide, Version 2.1. Zurich, Switzerland, ReSe and RSL.

Schläpfer, D. and R. Richter (2002). "Geo-atmospheric processing of airborne imaging spectrometry data. Part 1: parametric orthorectification." International Journal of Remote Sensing **23**: 2609-2630.